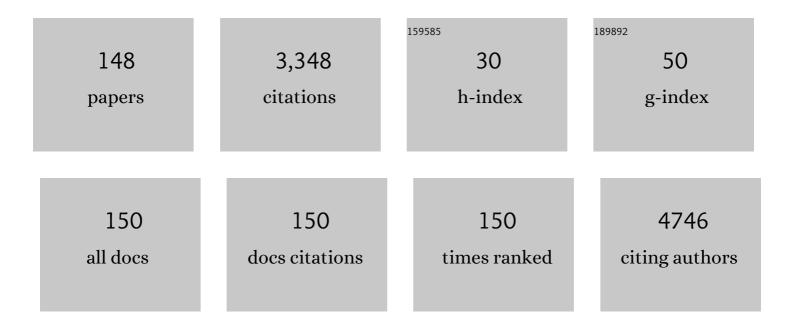
List of Publications by Year in descending order

Source: https://exaly.com/author-pdf/5192998/publications.pdf Version: 2024-02-01



#	Article	IF	CITATIONS
1	Hydrogen peroxide LSPR sensing with unoxidised CuNPs-Tween® 60. Journal of Materials Science, 2022, 57, 1714.	3.7	0
2	Green Silver Nanoparticles Promote Inflammation Shutdown in Human Leukemic Monocytes. Materials, 2022, 15, 775.	2.9	7
3	Solid Lipid Nanoparticles Administering Antioxidant Grape Seed-Derived Polyphenol Compounds: A Potential Application in Aquaculture. Molecules, 2022, 27, 344.	3.8	9
4	High Doses of Silica Nanoparticles Obtained by Microemulsion and Green Routes Compromise Human Alveolar Cells Morphology and Stiffness Differently. Bioinorganic Chemistry and Applications, 2022, 2022, 1-23.	4.1	4
5	Tailoring sheet resistance through laser fluence and study of the critical impact of a V-shaped plasma plume on the properties of PLD-deposited DLC films for micro-pattern gaseous detector applications. Diamond and Related Materials, 2022, 124, 108909.	3.9	3
6	Thermal neutron conversion by high purity 10B-enriched layers: PLD-growth, thickness-dependence and neutron-detection performances. European Physical Journal Plus, 2022, 137, 1.	2.6	2
7	From GO to rGO: An analysis of the progressive rippling induced by energetic ion irradiation. Applied Surface Science, 2022, 586, 152789.	6.1	14
8	Proton beam dosimetry based on the graphene oxide reduction and Raman spectroscopy. Vacuum, 2022, 201, 111113.	3.5	5
9	Copper Dependent Modulation of α-Synuclein Phosphorylation in Differentiated SHSY5Y Neuroblastoma Cells. International Journal of Molecular Sciences, 2021, 22, 2038.	4.1	9
10	Cyto/Biocompatibility of Dopamine Combined with the Antioxidant Grape Seed-Derived Polyphenol Compounds in Solid Lipid Nanoparticles. Molecules, 2021, 26, 916.	3.8	27
11	Structural and spectroscopic investigations on graphene oxide foils irradiated by ion beams for dosimetry application. Vacuum, 2021, 188, 110185.	3.5	20
12	Surface architecture of Neisseria meningitidis capsule and outer membrane as revealed by atomic force microscopy. Research in Microbiology, 2021, 172, 103865.	2.1	0
13	Synergistic Effect Induced by Gold Nanoparticles with Polyphenols Shell during Thermal Therapy: Macrophage Inflammatory Response and Cancer Cell Death Assessment. Cancers, 2021, 13, 3610.	3.7	13
14	Essential Oil-Loaded NLC for Potential Intranasal Administration. Pharmaceutics, 2021, 13, 1166.	4.5	13
15	Structural phase modifications induced by energetic ion beams in graphene oxide. Vacuum, 2021, 193, 110513.	3.5	7
16	Enhanced adsorption capacity of porous titanium dioxide nanoparticles synthetized in alkaline sol. Applied Physics A: Materials Science and Processing, 2020, 126, 1.	2.3	15
17	Plasmonic Light Trapping in Titania–Silver Dots Thin Films. Physica Status Solidi (B): Basic Research, 2020, 257, 2070035.	1.5	0
18	Ferulic Acid-NLC with Lavandula Essential Oil: A Possible Strategy for Wound-Healing?. Nanomaterials, 2020. 10. 898.	4.1	30

#	Article	IF	CITATIONS
19	Plasmonic Light Trapping in Titania–Silver Dots Thin Films. Physica Status Solidi (B): Basic Research, 2020, 257, 2000124.	1.5	0
20	Effect of temperature on the physical, optical and photocatalytic properties of TiO2 nanoparticles. SN Applied Sciences, 2020, 2, 1.	2.9	16
21	Investigations on graphene oxide for ion beam dosimetry applications. Vacuum, 2020, 178, 109451.	3.5	22
22	TiO 2 films by solâ€gel spinâ€coating deposition with microbial antiadhesion properties. Surface and Interface Analysis, 2019, 51, 1351-1358.	1.8	6
23	Wavelength, fluence and substrate-dependent room temperature pulsed laser deposited B-enriched thick films. Applied Surface Science, 2019, 483, 1044-1051.	6.1	5
24	A silver nanoparticle-poly(methyl methacrylate) based colorimetric sensor for the detection of hydrogen peroxide. Heliyon, 2019, 5, e02887.	3.2	19
25	Photochromic properties in silver-doped titania nanoparticles. Materials Research Express, 2019, 6, 036206.	1.6	3
26	Copper and ceruloplasmin dyshomeostasis in serum and cerebrospinal fluid of multiple sclerosis subjects. Biochimica Et Biophysica Acta - Molecular Basis of Disease, 2018, 1864, 1828-1838.	3.8	30
27	Highly sensitive conformational switching of ethane-bridged mono-zinc bis-porphyrin as an application tool for rapid monitoring of aqueous ammonia and acetone. Sensors and Actuators B: Chemical, 2018, 257, 685-691.	7.8	5
28	Calcite-forming <i>Bacillus licheniformis</i> Thriving on Underwater Speleothems of a Hydrothermal Cave. Geomicrobiology Journal, 2018, 35, 804-817.	2.0	8
29	Colloidal solution of silver nanoparticles for label-free colorimetric sensing of ammonia in aqueous solutions. Beilstein Journal of Nanotechnology, 2018, 9, 499-507.	2.8	17
30	The tale of Henry VII: a multidisciplinary approach to determining the post-mortem practice. Archaeological and Anthropological Sciences, 2017, 9, 1215-1222.	1.8	3
31	Enhanced electrical conductivity of collagen films through long-range aligned iron oxide nanoparticles. Journal of Colloid and Interface Science, 2017, 501, 185-191.	9.4	40
32	A simple approach to synthetize folic acid decorated magnetite@SiO ₂ nanostructures for hyperthermia applications. Journal of Materials Chemistry B, 2017, 5, 7547-7556.	5.8	16
33	Design and Synthesis of Ironâ€Doped Nanostructured TiO ₂ and Its Potential Use in the Photodegration of Hazardous Materials Present in Personal Care Products. ChemistrySelect, 2017, 2, 5095-5099.	1.5	3
34	Synthesis and Characterization of Mixed Iron-Manganese Oxide Nanoparticles and Their Application for Efficient Nickel Ion Removal from Aqueous Samples. Journal of Analytical Methods in Chemistry, 2017, 2017, 1-9.	1.6	15
35	Innovative hybrid vs polymeric nanocapsules: The influence of the cationic lipid coating on the "4S― Colloids and Surfaces B: Biointerfaces, 2016, 141, 450-457.	5.0	28
36	Promising Piezoelectric Properties of New ZnO@Octadecylamine Adduct. Journal of Physical Chemistry C, 2015, 119, 20143-20149.	3.1	27

#	Article	IF	CITATIONS
37	A Comparative Study of Pottery from Mersin-Yumuktepe and Arslantepe, Turkey. Archaeological Discovery, 2015, 03, 15-25.	0.5	0
38	Nondestructive Analysis of Silver Coins Minted in Taras (South Italy) between the V and the III Centuries BC. Journal of Archaeology, 2014, 2014, 1-12.	0.5	6
39	Solid-to-solid phase transformations of nanostructured selenium-tin thin films induced by thermal annealing in oxygen atmosphere. , 2014, , .		11
40	Cytotoxicity of \hat{I}^2 -D-glucose coated silver nanoparticles on human lymphocytes. AIP Conference Proceedings, 2014, , .	0.4	13
41	Highly selective hydrogenation of quinolines promoted by recyclable polymer supported palladium nanoparticles under mild conditions in aqueous medium. Applied Catalysis A: General, 2014, 481, 89-95.	4.3	64
42	The critical role of didodecyldimethylammonium bromide on physico-chemical, technological and biological properties of NLC. Colloids and Surfaces B: Biointerfaces, 2014, 121, 1-10.	5.0	35
43	Green synthesis of sucralose-capped silver nanoparticles for fast colorimetric triethylamine detection. Sensors and Actuators B: Chemical, 2013, 178, 1-9.	7.8	88
44	Controlled synthesis and chain-like self-assembly of silver nanoparticles through tertiary amine. Colloids and Surfaces A: Physicochemical and Engineering Aspects, 2013, 417, 10-17.	4.7	14
45	Interaction of pH-sensitive non-phospholipid liposomes with cellular mimetic membranes. Biomedical Microdevices, 2013, 15, 299-309.	2.8	22
46	Silver and carbon nanoparticles toxicity in sea urchin Paracentrotus lividus embryos. BioNanoMaterials, 2013, 14, .	1.4	13
47	Magnetostatic Field System for Uniform Cell Cultures Exposure. PLoS ONE, 2013, 8, e72341.	2.5	5
48	High ordered biomineralization induced by carbon nanoparticles in the sea urchin <i>Paracentrotus lividus</i> . Nanotechnology, 2012, 23, 495104.	2.6	14
49	Synthesis and growth mechanism of dendritic Cu2â^'xSe microstructures. Journal of Alloys and Compounds, 2012, 538, 8-10.	5.5	34
50	Role of the Cellular Prion Protein in the Neuron Adaptation Strategy to Copper Deficiency. Cellular and Molecular Neurobiology, 2012, 32, 989-1001.	3.3	13
51	Photofunctional multilayer films by assembling naked silver nanoparticles and a tailored nitric oxide photodispenser at water/air interface. Journal of Colloid and Interface Science, 2012, 368, 191-196.	9.4	15
52	Nanographite assembled films for sensitive NO2 detection. Sensors and Actuators B: Chemical, 2012, 161, 359-365.	7.8	9
53	Stress response induced by carbon nanoparticles in Paracentrotus lividus. International Journal of Molecular and Cellular Medicine, 2012, 1, 30-8.	1.1	9
54	Characterization of Composite Phthalocyanine–Fatty Acid Films from the Air/Water Interface to Solid Supports. Journal of Physical Chemistry B, 2011, 115, 14956-14962.	2.6	3

#	Article	IF	CITATIONS
55	Single step synthesis of SnO2–SiO2 core–shell microcables. Journal of Crystal Growth, 2011, 330, 22-29.	1.5	5
56	Synthesis and <i>in vitro</i> Cytotoxicity of Glycans-Capped Silver Nanoparticles. Nanomaterials and Nanotechnology, 2011, 1, 10.	3.0	14
57	Nanoclustering in Silicon Induced by Oxygen Ions Implanted. Nanomaterials and Nanotechnology, 2011, 1, 16.	3.0	0
58	Optical, morphological and structural characterization of Langmuir–Schaefer films of a functionalized copper phthalocyanine. Journal of Colloid and Interface Science, 2011, 363, 199-205.	9.4	6
59	Electronic properties of individual and assembled homotype SWCNT bundles. Chemical Physics Letters, 2011, 509, 152-157.	2.6	3
60	Aligned selenium microtubes array: Synthesis, growth mechanism and photoelectrical properties. Chemical Physics Letters, 2011, 510, 87-92.	2.6	5
61	SERS based optical sensor to detect prion protein in neurodegenerate living cells. Sensors and Actuators B: Chemical, 2011, 156, 479-485.	7.8	16
62	Aligning Singleâ€Walled Carbon Nanotubes By Means Of Langmuir–Blodgett Film Deposition: Optical, Morphological, and Photoâ€electrochemical Studies. Advanced Functional Materials, 2010, 20, 2481-2488.	14.9	70
63	Assembly of hybrid silver–titania thin films for gas sensors. Sensors and Actuators B: Chemical, 2010, 145, 794-799.	7.8	11
64	Shape-dependent plasmon resonances of Ag nanostructures. Superlattices and Microstructures, 2010, 47, 66-71.	3.1	11
65	Unusual coin from the Parabita hoard: combined use of surface and micro-analytical techniques for its characterisation. Journal of Cultural Heritage, 2010, 11, 233-238.	3.3	3
66	Monitoring prion protein expression in complex biological samples by SERS for diagnostic applications. Nanotechnology, 2010, 21, 165502.	2.6	21
67	Characterization and Growth Mechanism of Selenium Microtubes Synthesized by a Vapor Phase Deposition Route. Crystal Growth and Design, 2010, 10, 4890-4897.	3.0	32
68	Green synthesis of silver nanoparticles with sucrose and maltose: Morphological and structural characterization. Journal of Non-Crystalline Solids, 2010, 356, 344-350.	3.1	118
69	Poly(vinyl alcohol) capped silver nanoparticles as localized surface plasmon resonance-based hydrogen peroxide sensor. Sensors and Actuators B: Chemical, 2009, 138, 625-630.	7.8	167
70	Self-assembling of micro-patterned titanium oxide films for gas sensors. Sensors and Actuators B: Chemical, 2009, 140, 563-567.	7.8	9
71	Self-assembly and branching of sucrose stabilized silver nanoparticles by microwave assisted synthesis: From nanoparticles to branched nanowires structures. Colloids and Surfaces A: Physicochemical and Engineering Aspects, 2009, 348, 205-211.	4.7	20
72	Non-functionalized silver nanoparticles for a localized surface plasmon resonance-based glucose sensor. Nanotechnology, 2009, 20, 165501.	2.6	56

#	Article	IF	CITATIONS
73	Self-Assembly of n-Diamond Nanocrystals Into Supercrystals. Crystal Growth and Design, 2009, 9, 1245-1249.	3.0	23
74	The influence of inulin addition on the morphological and structural properties of durum wheat pasta. International Journal of Food Science and Technology, 2009, 44, 2218-2224.	2.7	36
75	WO3 gas sensors prepared by thermal oxidization of tungsten. Sensors and Actuators B: Chemical, 2008, 133, 321-326.	7.8	175
76	A new amperometric nanostructured sensor for the analytical determination of hydrogen peroxide. Biosensors and Bioelectronics, 2008, 24, 1057-1063.	10.1	197
77	Atomic force acoustic microscopy characterization of nanostructured selenium–tin thin films. Superlattices and Microstructures, 2008, 44, 641-649.	3.1	35
78	Synthesis and characterization of starch-stabilized Ag nanostructures for sensors applications. Journal of Non-Crystalline Solids, 2008, 354, 5515-5520.	3.1	70
79	Photoconductivity of Packed Homotype Bundles Formed by Aligned Single-Walled Carbon Nanotubes. Nano Letters, 2008, 8, 968-971.	9.1	13
80	Iris revolutaColas., natural hybrid origin species: characterization and preservation problems. Plant Biosystems, 2008, 142, 162-165.	1.6	0
81	Characterization of ablation plasma ion implantation. Nuclear Instruments & Methods in Physics Research B, 2005, 240, 36-39.	1.4	9
82	Meso- and nano-scale investigation of carbon fibers coated by nano-crystalline diamond. Chemical Physics Letters, 2005, 402, 340-345.	2.6	15
83	Precipitation of superstructured nano-crystals in high-dose implanted Si: an XHRTEM study. Journal Physics D: Applied Physics, 2004, 37, 2730-2736.	2.8	14
84	Organized networks of helically wound single-walled C-nanotubes. Chemical Physics Letters, 2004, 388, 36-39.	2.6	11
85	Morphological, structural and electrical characterization of nanostructured vanadium–tin mixed oxide thin films. Journal of Non-Crystalline Solids, 2004, 341, 68-76.	3.1	10
86	High-resolution electron microscopy of Zn- and Bi-related superlattices in ion implanted (1 0 0) Si. Journal of Materials Science: Materials in Electronics, 2003, 14, 783-786.	2.2	0
87	Organization of single-walled nanotubes into macro-sized rectangularly shaped ribbons. Chemical Physics Letters, 2003, 381, 86-93.	2.6	18
88	Aligned arrays of carbon nanotubes: modulation of orientation and selected-area growth. Chemical Physics Letters, 2003, 367, 109-115.	2.6	39
89	Synthesis and Characterization of TiO2Nanocrystals Prepared fromn-Octadecylamineâ~'Titanyl Oxalate Langmuirâ 'Blodgett Films. Langmuir, 2003, 19, 3486-3492.	3.5	23
90	Modulation of charge transport in diamond-based layers. Journal of Applied Physics, 2003, 94, 416-422.	2.5	11

#	Article	IF	CITATIONS
91	Effects of hydrogen diffusion and UV irradiation in Pd thin films. , 2003, , .		Ο
92	<title>Performance study of hydrogen effect in Pd thin films irradiated by a UV irradiation</title> . , 2003, 5147, 185.		0
93	Characterization of African dust over southern Italy. Atmospheric Chemistry and Physics, 2003, 3, 2147-2159.	4.9	81
94	Temperature and ion flux dependence of damage structures in Zn+ implanted and laser annealed GaAs. Journal Physics D: Applied Physics, 2002, 35, 2830-2836.	2.8	0
95	Physical properties of sputtered molybdenum oxide thin films suitable for gas sensing applications. Journal Physics D: Applied Physics, 2002, 35, 228-233.	2.8	30
96	LB multilayers of highly conjugated porphyrin dimers: differentiation of properties and behaviour between the free base and the metallated derivatives. Colloids and Surfaces A: Physicochemical and Engineering Aspects, 2002, 198-200, 897-904.	4.7	16
97	Analysis of nuclear transmutations observed in D- and H-loaded Pd films. International Journal of Hydrogen Energy, 2002, 27, 527-531.	7.1	4
98	Study of Gas Sensing Performances of Langmuirâ^'Blodgett Films Containinig an Alkyne-Linked Conjugated-Porphyrin Dimer. Langmuir, 2001, 17, 8139-8144.	3.5	22
99	Structural and electrical properties of In2O3/SeO2thin films for gas-sensing applications. Journal Physics D: Applied Physics, 2001, 34, 2097-2102.	2.8	33
100	Ion-Beam-Assisted Nanocrystal Formation in Silicon Implanted with High Doses of Pb+and Bi+Ions. Japanese Journal of Applied Physics, 2001, 40, 5841-5849.	1.5	5
101	Temperature-dependent conduction of W-containing composite diamond films. Applied Physics Letters, 2001, 79, 2007-2009.	3.3	6
102	Growth of single-walled carbon nanotubes by a novel technique using nanosized graphite as carbon source. Chemical Physics Letters, 2000, 327, 284-290.	2.6	25
103	Structural and electrical properties of In2O3–SeO2 mixed oxide thin films for gas sensing applications. Journal of Applied Physics, 2000, 88, 6571-6577.	2.5	35
104	High resolution transmission electron microscopy of elevated temperature Zn+ implanted and low-power pulsed laser annealed GaAs. Journal of Applied Physics, 2000, 88, 1806-1810.	2.5	12
105	Structural reordering and electrical activation of ion-implanted GaAs and InP due to laser annealing in a controlled atmosphere. Physical Review B, 1999, 59, 2986-2994.	3.2	11
106	Thermal deposition and characterisation of In–Se mixed oxides thin films for NO gas sensing applications. Sensors and Actuators B: Chemical, 1999, 58, 356-359.	7.8	8
107	Comparative optical and morphological investigation of meso,meso′-buta-1,3-diyne-bridged Cu(II) octaethyl porphyrin dimer Langmuir–Blodgett films. Materials Science and Engineering C, 1999, 8-9, 107-111.	7.3	3
108	Gas sensing properties of meso,meso′-buta-1,3-diyne-bridged Cu(II) octaethylporphyrin dimer Langmuir–Blodgett films. Sensors and Actuators B: Chemical, 1999, 57, 179-182.	7.8	12

#	Article	IF	CITATIONS
109	Synthesis and characterization of ZnS nanoparticles in water/AOT/n-heptane microemulsions. Applied Physics A: Materials Science and Processing, 1999, 69, 369-373.	2.3	70
110	Sputter deposition of tungsten trioxide for gas sensing applications. Journal of Materials Science: Materials in Electronics, 1998, 9, 317-322.	2.2	19
111	Gas-sensing properties of porphyrin dimer Langmuir–Blodgett films. Thin Solid Films, 1998, 327-329, 341-344.	1.8	41
112	Physical Properties of Molybdenum Oxide Thin Films for NO Gas Detection. Physica Status Solidi A, 1998, 168, 249-256.	1.7	32
113	Physical and structural characterization of tungsten oxide thin films for NO gas detection. Thin Solid Films, 1998, 324, 44-51.	1.8	94
114	Langmuir-Blodgett films of a phthalocyanine symmetrically functionalized with eight ester units. Materials Science and Engineering C, 1998, 5, 317-320.	7.3	9
115	Kinetic behavior analysis of porphyrin Langmuir–Blodgett films for conductive gas sensors. Journal of Applied Physics, 1998, 84, 1416-1420.	2.5	44
116	Thermal deposition and characterization of Se-Sn mixed oxide thin films for NO gas sensing applications. Journal of Applied Physics, 1998, 83, 3541-3546.	2.5	22
117	Physical Properties of Molybdenum Oxide Thin Films for NO Gas Detection. Physica Status Solidi A, 1998, 168, 249-256.	1.7	2
118	Gas-sensing properties of sputtered thin films of tungsten oxide. Journal Physics D: Applied Physics, 1997, 30, 3211-3215.	2.8	42
119	Structural and electrical properties of sputtered vanadium oxide thin films for applications as gas sensing material. Journal of Applied Physics, 1997, 81, 2709-2714.	2.5	56
120	Titanium oxide thin films for NH3 monitoring: Structural and physical characterizations. Journal of Applied Physics, 1997, 82, 54-59.	2.5	69
121	Porphyrin Dimers Linked by a Conjugated Alkyne Bridge:  Novel Moieties for the Growth of Langmuirâ~'Blodgett Films and Their Applications in Gas Sensors. Langmuir, 1997, 13, 5951-5956.	3.5	49
122	Gas-sensing properties of multilayers of two new macrocyclic copper complexes. Sensors and Actuators B: Chemical, 1997, 44, 585-589.	7.8	8
123	Langmuir-Blodgett films of Cu(II)-tetrakis (3,3-dimethylbutoxycarbonyl) phthalocyanine: a spectrophotometric and TEM analysis of their structure and morphology. Thin Solid Films, 1996, 280, 249-255.	1.8	28
124	Crossâ€sectional high resolution electron microscopy of Zn+ implanted and lowâ€power pulsedâ€laser annealed GaAs. Applied Physics Letters, 1996, 69, 4072-4074.	3.3	15
125	Metalorganic vapour phase epitaxy growth of ZnS layers by (t-Bu)SH and Me2Zn:Et3N precursors. Journal of Crystal Growth, 1995, 156, 45-51.	1.5	15
126	Physical characterization of In2Se3 thin films prepared by electron beam evaporation. Vacuum, 1995, 46, 997-1000.	3.5	13

#	Article	IF	CITATIONS
127	Surface structural and morphological characterization of ZnTe epilayers grown on {100} GaAs by MOVPE. Journal of Crystal Growth, 1993, 128, 633-638.	1.5	13
128	Growth and characterization of tin oxide thin films prepared by reactive sputtering. Solar Energy Materials and Solar Cells, 1993, 31, 235-242.	6.2	12
129	Structural and morphological analysis of reactively sputtered tellurium suboxide thin films. Journal of Non-Crystalline Solids, 1993, 155, 67-76.	3.1	5
130	Convergent beam electron diffraction study of extended defects in gallium chalcogenide single crystals grown from the melt. Semiconductor Science and Technology, 1992, 7, A122-A126.	2.0	2
131	Size-dependent lattice contraction inCdS1â^'xSexnanocrystals embedded in glass observed by Raman scattering. Physical Review B, 1992, 45, 13792-13795.	3.2	136
132	Structural characterization of hydrogenated amorphous GaAs. Journal of Non-Crystalline Solids, 1992, 151, 253-260.	3.1	5
133	Structural characterization of unhydrogenated amorphous GaAs. Journal of Non-Crystalline Solids, 1991, 127, 12-18.	3.1	14
134	<title>Optical investigation of microcrystals in glasses</title> ., 1991, 1513, 130.		1
135	Analysis of extended defects in melt-grown GaSe single crystals by convergent-beam electron diffraction techniques. Ultramicroscopy, 1991, 35, 71-76.	1.9	1
136	Convergent-beam electron diffraction analysis of GaSe crystals grown from the melt by different doping elements. Nuovo Cimento Della Societa Italiana Di Fisica D - Condensed Matter, Atomic, Molecular and Chemical Physics, Biophysics, 1991, 13, 233-245.	0.4	4
137	Correlation between the structural and optical properties of polydispersed Il–VI quantum dots in glass matrix. Journal of Applied Physics, 1991, 70, 6898-6901.	2.5	19
138	Convergent-beam electron diffraction characterization of dislocations in GaS single crystals. Ultramicroscopy, 1990, 33, 143-149.	1.9	3
139	Study of the polytypism in melt grown InSe single crystals by convergent beam electron diffraction. Journal of Crystal Growth, 1990, 100, 347-353.	1.5	13
140	Characterization of CdS epitaxial films by high energy reflected electrons. Journal of Crystal Growth, 1990, 101, 185-189.	1.5	0
141	CBED analysis of extended defects in melt-grown GaSe single crystals. Proceedings Annual Meeting Electron Microscopy Society of America, 1990, 48, 494-495.	0.0	Ο
142	Convergent-beam electron diffraction study of melt-and vapour-grown single crystals of gallium chalcogenides. Nuovo Cimento Della Societa Italiana Di Fisica D - Condensed Matter, Atomic, Molecular and Chemical Physics, Biophysics, 1989, 11, 1145-1163.	0.4	15
143	Electron diffraction study of In2Se3 melt grown crystals. Journal of Crystal Growth, 1989, 96, 947-952.	1.5	2
144	Optical absorption and structure of thermally annealed gallium selenide thin films. Journal of Applied Physics, 1989, 65, 1164-1167.	2.5	21

#	Article	IF	CITATIONS
145	Numerical evaluation of lattice parameters from high-order Laue zone lines in convergent-beam electron diffraction disks. Ultramicroscopy, 1988, 26, 377-384.	1.9	3
146	Effects of thermal annealing on optical absorption of amorphous indium selenide thin films. Solar Energy Materials and Solar Cells, 1987, 15, 209-218.	0.4	44
147	Electron diffraction study of melt-grown InSe crystals. Nuovo Cimento Della Societa Italiana Di Fisica D - Condensed Matter, Atomic, Molecular and Chemical Physics, Biophysics, 1986, 7, 795-806.	0.4	16
148	Characterization of Pd-H/sub 2/ thin films irradiated by UV laser. , 0, , .		0